Archives of Gerontology and Geriatrics 83 (2019) 328–337

Contents lists available at ScienceDirect

Archives of Gerontology and Geriatrics

journal homepage: www.elsevier.com/locate/archger

# Spatial-temporal analysis of tuberculosis in the geriatric population of China: An analysis based on the Bayesian conditional autoregressive model

Endawoke Amsalu[a,b], Mengyang Liu[a,b], Qihuan Li[a,b], Xiaonan Wang[a,b], Lixin Tao[a,b], Xiangtong Liu[a,b], Yanxia Luo[a,b], Xinghua Yang[a,b], Yingjie Zhang[c], Weimin Li[d], Xia Li[e], Wei Wang[f], Xiuhua Guo[a,b,*]

[a] *Department of Epidemiology and Health Statistics, School of Public Health, Capital Medical University, Beijing, 100069, China*
[b] *Beijing Municipal Key Laboratory of Clinical Epidemiology, Beijing, 100069, China*
[c] *Chinese Center for Disease Control and Prevention, Beijing, 102206, China*
[d] *Beijing Chest Hospital, Beijing, 101149, China*
[e] *Department of Mathematics and Statistics, La Tribe University, Melbourne, 3086, Australia*
[f] *Global Health and Genomics, School of Medical Sciences and Health, Edith Cowan University, Joondalup, Perth, WA6027, Australia*

A R T I C L E I N F O

*Keywords:*
TB
Bayesian
Spatial
Spatial-temporal
Elderly

A B S T R A C T

*Background:* Tuberculosis (TB) remains a clinical and epidemiological challenge in the geriatric population. We aim to examine the spatial-temporal pattern of TB in the geriatric population and its relationship with meteorological & sociodemographic factors using the Bayesian conditional autoregressive (CAR) model.
*Method:* An ecological design was used in the geriatric (age > = 65 years) population from 2005 to 2015. Spatial autocorrelation and hot spots were explored using geographical information system (GIS) statistics. The Bayesian CAR model was used for modeling TB to estimate the parameters using the WinBUGS software. Deviance information criteria (DIC) were used to select the best performing model.
*Results:* Spatially, TB was clustered in Central China and southeast of China. Temporally, an increasing trend and high peak of TB was detected during the spring. TB was significantly associated with air temperature at the posterior mean: -0.165 (95%CI: -0.235, -0.108), and it was negatively associated with average wind speed: -0.028 (95%CI: -0.043, -0.018) and positively associated with rainfall: 0.095 (95%CI: 0.045, 0.163). TB was significantly and positively associated with population density: 0.088(95%CI: 0.031, 0.129) and sex ratio (M: F): 0.162 (95%CI: 0.091, 0.284) and was negatively related with gross domestic product (GDP): -0.046(95%CI: -0.156, -0.037). Out of 31 provinces, 17 provinces had a higher risk for TB.
*Conclusion:* TB shows a clear spatial and seasonal variation; it is geographically aggregated, and more men are affected than women. Areas with an underprivileged economy, high population density, high rainfall, low wind speed, and low temperature have a higher risk for TB.

## 1. Introduction

TB is a disease caused by bacteria that are spread from person to person (CDC, 2016) and continues to be a leading cause of disease and death worldwide; TB has more than 50% burden in five countries: India, Indonesia, China, Philippines, and Pakistan (WHO, 2017).

It is stated and recognized that the elderly are vulnerable to developing and succumbing to TB diseases (Schaaf et al., 2010; Ito, 2013; Toyota and Sasaki, 2010). Along with the geriatric population growth in numbers, TB is an increasing problem in many countries (Hussein et al., 2013; World Health Organization, 2010; Menezes et al., 2007; Pratt et al., 2011) because of the age-related decline in immunity (Rieder, 1999), increasing longevity (Davies, 2007), poverty (Rieder, 1999), malnutrition (Jovic, 2001) and tobacco smoking (Petersen, 2003), which are proven risk factors. Although TB in the elderly is a preventable disease, patients have a higher chance of unfavorable outcomes due to drug-related adverse events, increased comorbidity, and poverty than young individuals (Ananthakrishnan et al., 2013; Velayutham et al., 2014). Globally, the death rate due to TB increases to 57% among people older than 50 years of age; of these, more than 50% of the deaths occur in those aged 65 years and older (IHME (Institute for Health Metrics and Evaluation), 2016). The proportion of death

* Corresponding author at: Department of Epidemiology and Health Statistics, School of Public Health, Capital Medical University, No.10 Xitoutiao, Youanmen Wai Street, Fengtai District, Beijing, 100069, PR China.
*E-mail address:* statguo@ccmu.edu.cn (X. Guo).

https://doi.org/10.1016/j.archger.2019.05.011
Received 25 October 2018; Received in revised form 18 April 2019; Accepted 12 May 2019
Available online 18 May 2019
0167-4943/ 

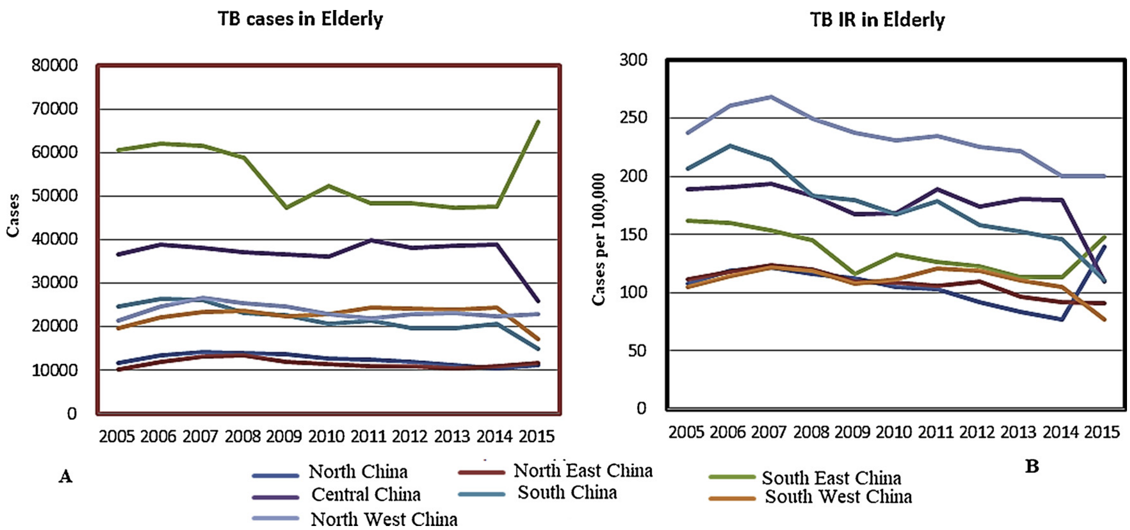


**Fig. 1.** A reported tuberculosis cases A) in the elderly and expressed as B) incidence rate per 100,000 people in China.from 2005 to 2015.

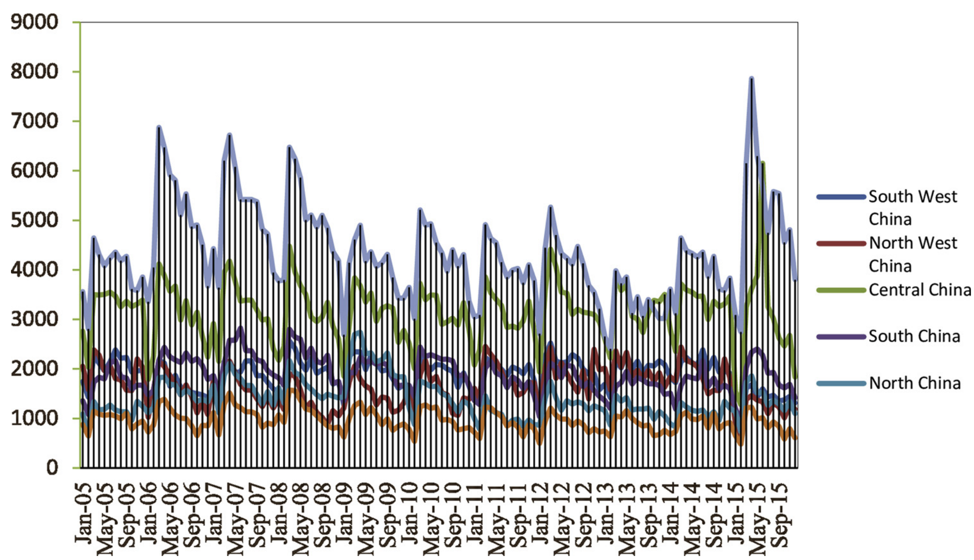


**Fig. 2.** Monthly distribution of tuberculosis cases in the elderly in China.2005–2015.

among individuals aged 50 years and older is highest in high-income countries (92% in Australia and 93% in Western Europe), East Asia (79%) and Tropical Latin America (65%) (IHME (Institute for Health Metrics and Evaluation), 2016). In India, the TB burden in the elderly is estimated to make up 14% of all TB cases with extra challenges due to the presence of drug-resistant strains of TB (Udwadia and Vendoti, 2013; Babu and Laxminarayan, 2012). In China, according to the 2010 national TB prevalence survey, the TB burden more than quadruples at an age of 75 years, and an age-associated increase in the burden was most pronounced in Chinese men (Technical Guidance Group of the Fifth National TB Epidemiological Survey and The Office of, Survey FNTE, 2012). A study in the Hunan Province of China showed that the prevalence of TB was more than twice as high in those aged 65 years and older than in adults younger than 64 years of age (Abuaku et al., 2010). The proportion of older people (aged > = 65 years) among reported patients with TB and deaths has gradually increased (Li et al., 2017). A recent TB survey in Shandong, a relatively industrialized province in China, found a much higher proportion(55%) of bacteriologically confirmed TB cases in the elderly, with a prevalence rate of 34 per 100,000 population (Zhang et al., 2015). TB in the aging population remains a clinical and epidemiological challenge. Although the life expectancy and TB burden in the elderly is expected to vary from region to region, the spatial epidemiology of TB in the elderly is understudied. Spatial epidemiology, therefore, has to consider both space and time (Pfeiffer et al., 2008). The Bayesian spatial method is useful in minimizing bias and variance compared to conventional statistical methods (Besag et al., 1991).

The spatial and temporal model provides spatial distribution and temporal changes of the relative risk of a disease across a study area. Most Bayesian methods propose extensions of the purely spatial models postulated by others; several spatial models have been proposed for TB and its risk determinants using the conditional autoregressive (CAR) model (Besag et al., 1991; Clayton and Kaldor, 1987; Knorr-Held and Besag, 1998; Waller et al., 1997; Da et al., 2012; Randremanana et al., 2010; De Queiroz Mello et al., 2006; Venkatesan, 2008; Venkatesan et al., 2012; Cao et al., 2016). However, several Bayesian methods postulated the spatial-temporal model in the general population and not in high-risk populations. Additionally, they did not include the sociodemographic and climate factors together. Therefore, the aim of this study is to examine the spatial-temporal patterns of TB specifically in the geriatric population and to evaluate its relationship to climate and sociodemographic factors using the CAR model.

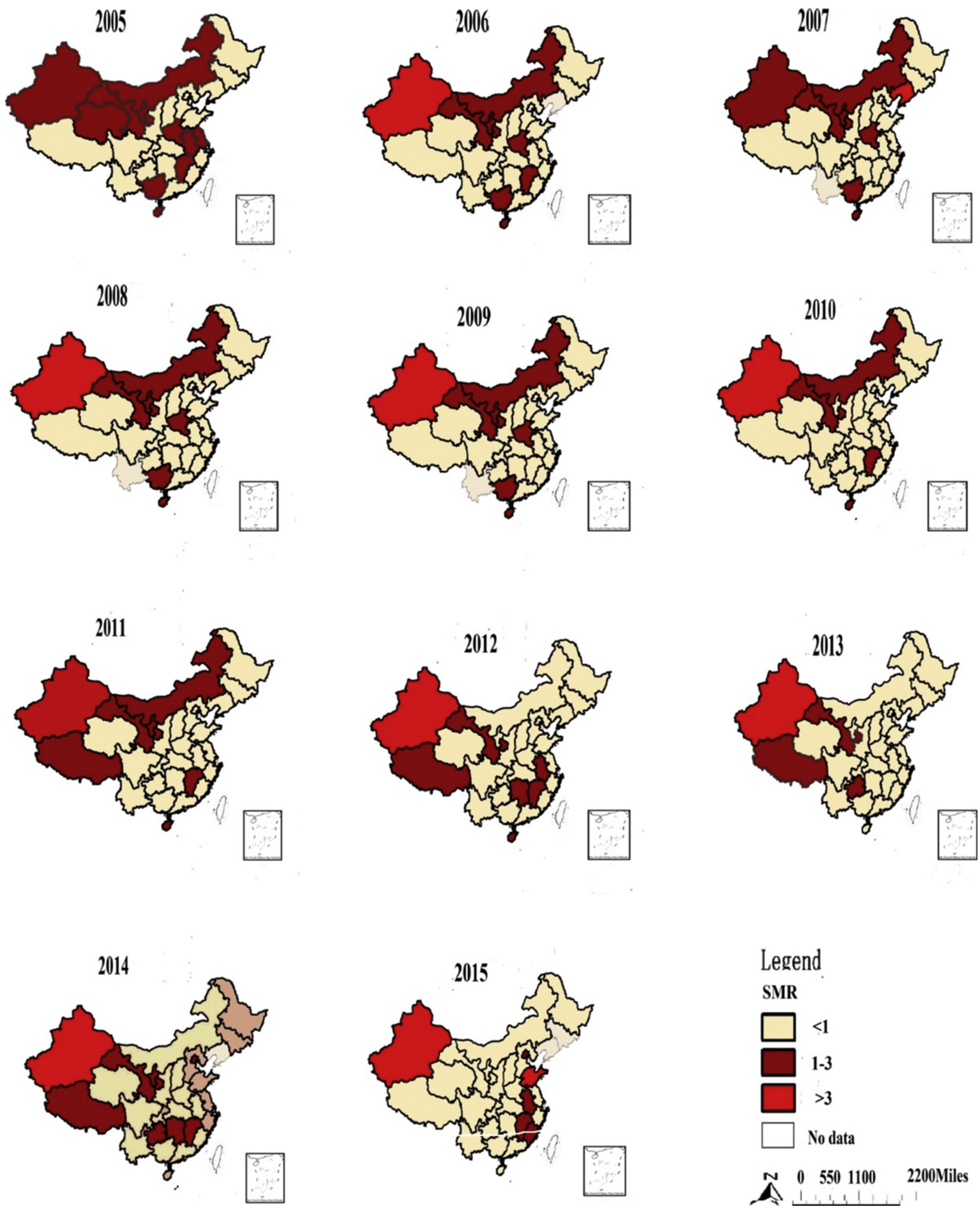


**Fig. 3.** The SMR (standardized morbidity ratio) for the spatial-temporal analysis of tuberculosis in the elderly in mainland China in 31 provinces.2005–2015.

## 2. Methods

### *2.1. Study design and population*

An ecological study was conducted in the geriatric population in mainland China in 31 provinces (excluding Hongkong, Maco, and Taiwan) from 2005 to 2015. The daily, monthly and yearly reported data of tuberculosis was extracted from the Chinese CDC. Population-level sociodemographic data such as growth domestic product (GDP), sex ratio, and population density were extracted from the National Bureau of Statistics of China. Meteorological data, such as average atmospheric pressure (kPa), average temperature (°C), relative humidity (percentage), average rainfall, and wind speed, were collected from the China Meteorological Data Sharing Service System.

### *2.2. Statistical analysis*

The overall crude incidence rate of TB in the elderly and the sex-

**Table 1**
Global spatial autocorrelation analysis of tuberculosis in the elderly population in China, 2005-2015.

| Years | Moran I | Z-Score | P-Value |
|---|---|---|---|
| 2005 | 0.146889 | 2.503134 | 0.01231 |
| 2006 | 0.093246 | 1.736311 | 0.08250 |
| 2007 | 0.081351 | 1.562712 | 0.11812 |
| 2008 | 0.072823 | 1.44598 | 0.14818 |
| 2009 | 0.087964 | 1.649842 | 0.01975 |
| 2010 | 0.054487 | 1.19155 | 0.23343 |
| 2011 | 0.104308 | 1.870015 | 0.06148 |
| 2012 | 0.119799 | 2.082695 | 0.03727 |
| 2013 | 0.133188 | 2.260162 | 0.02381 |
| 2014 | 0.14494 | 2.421347 | 0.01546 |
| 2015 | 0.142388 | 2.380347 | 0.01729 |

and residence-adjusted standardized morbidity ratio (SMR) was calculated for each region/province. Spatial autocorrelation was explored on a global scale using Moran's I statistic and on a local scale using local indicators of spatial association (LISA), and it was estimated using the Anselin Local Moran's I statistic and the Getis-Ord Gi* statistic using ArcGIS. We used the hierarchical Bayesian CAR model analysis based on MCMC simulation for modeling TB disease and estimated the parameters using WinBUGS software. TB cases in the elderly is considered count data; thus, the observed number ($O_i$) of cases was assumed to follow a Poisson distribution. Based on this assumption, six models were constructed as follows: **Model 1**: a model with no spatial autocorrelation; hence, it was assumed to be without spatial effect (uncorrelated random effect); **Model 2**: a model considering an autoregressive temporal effect ($g_i$); **Model 3**: a model considering a temporal trend and autoregressive temporal effect (a1*time); **Model 4**: a model considering a spatially structured random effect (correlated random effect) to detect potential spatial dependency; **Model 5**: a model considering correlated (**CH**) and uncorrelated (**UH**) spatial random effects and temporal and autoregressive time effects; and **Model 6**: a model considering a spatial temporal interaction (Psi), spatial **CH** and **UH** spatial random effects, temporal dependence, and autoregressive time effect. The final full model is written below. This model assumed that the observed number of TB cases (O) for the ith province ($i$ = 1–31) for the year $j$ ($j$ = 2013–2015) followed a Poisson distribution with a mean ($\mu$):

$$O_{ij} \sim Poisson(\mu_{ij}),$$

$$\log(\mu_{ij}) = \log(e_i) + \theta_{ij},$$

$$\theta_{ij} = \exp(\alpha_0 + \alpha_1 time_j + u_i + v_i + g_j + psi_{ij} + \sum_{n=1}^{p} \beta_n X_n)$$

Where $\alpha_0$denoted intercept; $e_{ij}$denoted expected number of the TB cases in the $j$th year in the $i$th region; $time_j$denoted the effect of the $j$th year; $\alpha_1$denoted the coefficient of the time; $u_i$denoted the effect of correlated spatial random effect in each province; $v_i$denoted the effect of uncorrelated spatial random effect in each province; $g_j$denoted the autoregressive time effect; $psi_{ij}$denoted the interaction of the spatial-temporal effect in each year in each province; and$X_n$denoted the covariates. $\beta_n$denoted the coefficient of the covariates for $i = 1, 2, \cdots, 31; j = 1, 2, \cdots, 11; n = 1, 2, \cdots, p$.

The spatially structured random effects were computed using the prior structure of CAR, which is defined using an adjacency matrix to determine the spatial relationships between provinces. The adjacency matrix for each province was generated using the WinBUGS tool after exporting the shape file of the China map in S-Plus format. To obtain the S-Plus format we used the map2 WinBUGS software. If two provinces were not neighbors, a weight of 0 was considered, and a weight of 1 was considered if two provinces were neighbors.

In this study, we selected the appropriate prior distribution for each parameter in our model based on previously published studies (Cao et al., 2016; Alene et al., 2017a).

A flat prior distribution was used as a noninformative improper prior with bounds -∞ and +∞ to the intercept(α). Prior probability distributions for the coefficients (β) were assumed to have normal distributions with a mean = 0 and a precision (i.e., the inverse of the variance) = $1 \times 10^{-}$ (Hussein et al., 2013). The unstructured random effects (υ_i) and spatially structured random effects ($\nu$_i) were assumed to have a mean of zero and a precision (the inverse of the variance) of 1/σu2 and 1/σv2, respectively. The priors for the precision of the unstructured and spatially structured random effects assigned a non-informative gamma distribution with a shape and scale parameters (0.05, 0.0005). A MCMC simulation approach with Gibbs sampling in WinBugs was used to infer the posterior parameters from the prior and data likelihood information. If the iterations of an MCMC before effective convergence are used to summarize the target distribution, they can yield incorrect inference. Therefore, the use of MCMC assumes convergence (the outcomes for a Gibbs sampler will eventually exhibit a stationary distribution). In this study, the convergence of the corresponding MCMC was monitored both graphically and numerically after we ran a single chain.

The models were run subsequently for 100,000 iterations, and the DIC was stored for the model selection, where a small value DIC indicated a preferred model. The model with a lower DIC value was considered as a best-fit model, and then the model ran by incorporating all the covariates(S1). In this study, for the best-fit models (Model IV), convergence occurred within the first 10,000 iterations. The model iteration process stopped when convergence of the posterior kernel densities and history plots occurred, and then the posterior distribution of each parameter was stored for the summary measures of the posterior mean, M.C. error, standard deviation and the 5% and 95% percentile interval (which is the 95% credible interval).

### 2.3. Sensitivity analysis

Sensitivity analysis was conducted to investigate the robustness of the results by considering commonly used prior distributions (inverse-gamma priors for the variance parameter, inverse gamma (0.001, 0.0001)) for precision unstructured and structured spatial random effects.

## 3. Results

During the study period, 2,015,927 TB cases were reported, and out of those cases, there were 1,496,844(74.25%) male patients. As per Fig. 1B, Southeast and Northeast China reported high and low numbers of cases, respectively. At province level, high and low numbers of cases were reported in Henan and Tibet province, respectively. The TB incidence in the geriatric population was 144 per 100,000 population for the period 2005–2015. The TB burden in the geriatric population showed a relative increase. The years 2005 and 2012 were the years where minimum and maximum numbers of TB cases were recorded, respectively (Fig. 1 A&B depict the trend of TB in the elderly).

### 3.1. Temporal patterns of TB cases in the elderly

Fig. 2 shows the monthly TB cases from 2005 to 2015. There was an evident trend variation: the maximum number of TB cases were registered in the spring (Mar-May) each year, which was followed by a volatile declining trend the following summer (June-August) and autumn (Sep-Nov); finally, the minimum number of cases were recorded in winter (Dec-Feb). The peak month for TB cases was March, and the number of cases declined gradually after April during the period 2005–2015.

The standardized morbidity ratio (SMR) of TB cases shows a spatial variation from province to province and year to year (Fig. 3). The

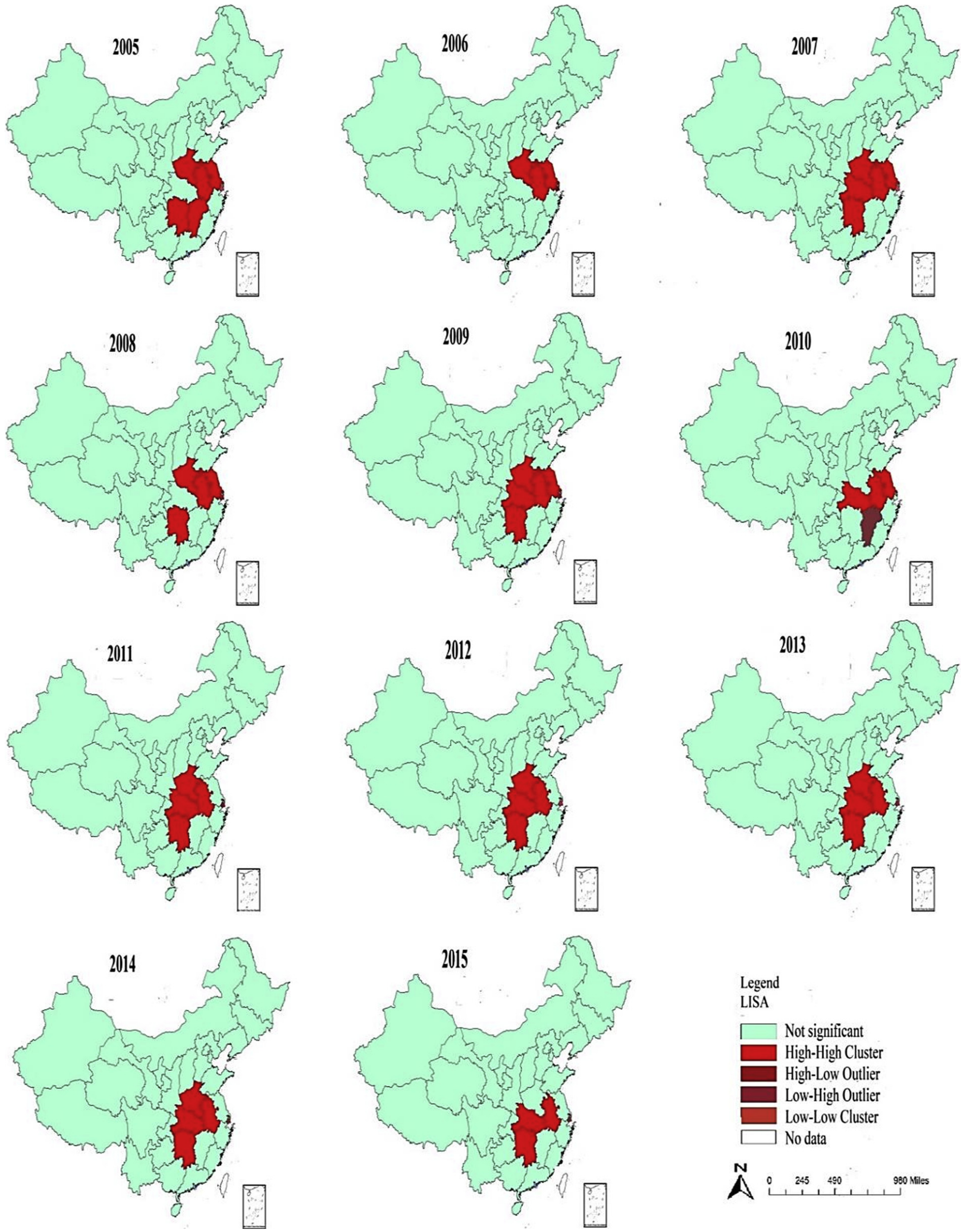


**Fig. 4.** The LISA cluster map of tuberculosis incidence in the elderly in mainland China.2005–2015.

pooled crude SMR indicated the highest TB morbidity in Northwest China, including Xinjiang, Gansu, and Haina; Tianjin, a city located in northern China, showed the lowest SMR compared to other provinces.

### 3.2. Spatial distribution of TB

The spatial autocorrelation (Global Moran's I) analysis of TB showed that the Global Moran's I value ranged from 0.054487 to 0.146889, and the Z-score peaked from 1.19155 to 2.503134 from 2005 to 2015. Therefore, the distribution of TB was spatially correlated in each study year, except in 2007 (Moran's I = 0.081351, P = 0.11812), 2008 (Moran's I = 0.072823, P = 0.148183) and 2010 (Moran's I = 0.054487, P = 0.233438); therefore, the TB incidence in the elderly indicated a lower likelihood that a clustered pattern of cases could be

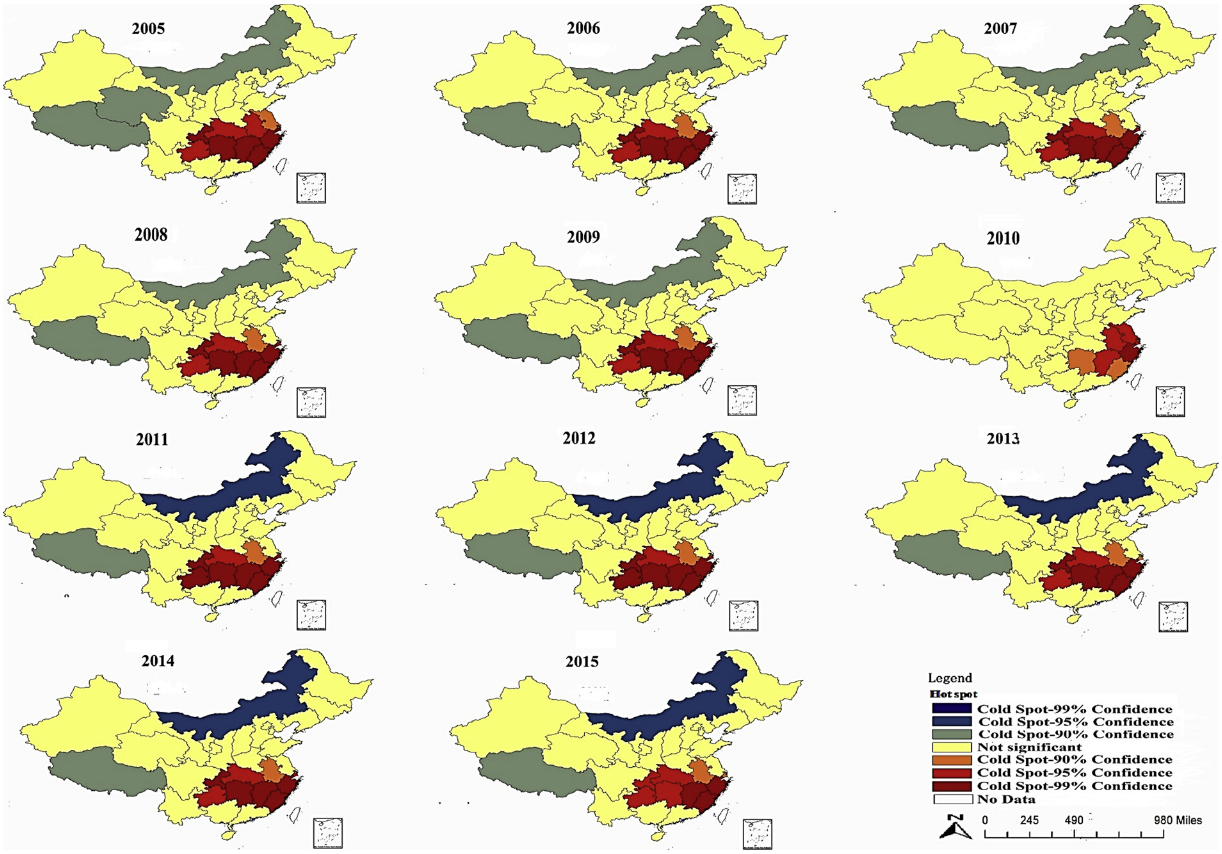


**Fig. 5.** The hot-spot analysis of Getis-Ord Gi* statistics for TB in the elderly in mainland China.2005–2015.

**Table 2**
Bayesian DIC values for tuberculosis in the elderly in mainland China in 31 Provinces, 2005-2015.

| Model | Hierarchical model structures | Dbar | Dhat | DIC* | pD |
|---|---|---|---|---|---|
| Model 1 | $\theta_{ij} = exp\ (a_0 + u_i)$ | 47640 | 47640 | 47600 | 47680 |
| Model 2 | $\theta_{ij} = exp\ (ao + u_i + g_i)$ | 36470 | 36410 | 36,520 | 53.95 |
| Model 3 | $\theta_{ij} = exp\ (ao + u_i + g_i + a_1 * t_i)$ | 36470 | 36410 | 36,520 | 54.16 |
| Model 4 | $\theta_{ij} = exp\ (a_0 + v_i + g_i + a_1 * t_i)$ | 36480 | 36510 | 36450 | −31.8 |
| Model 5 | $\theta_{ij} = exp\ (a_0 + v_i + g_i + a_1 * t_i + u_i)$ | 36460 | 57660 | 15260 | −2120 |
| Model 6 | $\theta_{ij} = exp\ (a_0 + v_i + g_i + a_1 * t_i + u_i + Ps_{ij})$ | 2242 | 2684 | 1800 | −442 |

$Ps_{ij} =$ spatial-temporal interaction effect.
$u_i =$ uncorrelated spatial random effect (no spatial dependency among the 31 provinces).
$v_i =$ correlated random spatial effect (spatial random effect in each of the 31 provinces).
$g_i =$ autoregressive time effect (from 2005 to 2015).
$t_i =$ time trend effect.[2005–2015]
* DIC = Deviance information criterion.

the result of random chance, and there was the presence of positive spatial autocorrelation and spatial dependency in mainland China (Table 1).

### 3.3. Local spatial autocorrelation analysis (LISA)

The Anselin Moran's I statistic (local spatial autocorrelation analysis) was further used to detect the significant TB clusters with the intensity of nearby clusters. Fig. 4 shows a statistically significant cluster of high values (HH), clusters of low values (LL), outliers in which a high value is surrounded mainly by low values (HL), and outliers in which a low value is surrounded mainly by high values (LH).

Spatial clustering was observed between neighboring provinces. The high-high positive spatial association of TB incidence was detected in Hunan, Hubei, Henan, Anhui and Jiangsu provinces in 2005, in Henan, Anhui and Jiangsu provinces in 2006, in Hunan, Anhui, and Jiangsu provinces, and Shanghai (mega-city of China) in 2009, and in Hunan, Anhui, and Jiangsu provinces in 2010-2015. Generally, high-high clusters of TB cases were detected in Central China and neighboring provinces (Fig. 4).

### 3.4. Hot spot Clustering (Getis-Ord Gi*)

A hot spot analysis using Getis-Ord Gi* was conducted to detect and display the statistically significant hot spots (clustering of high values) and cold spots (clustering of low values). The score of Giz > 2.58 reflects the presence of disease aggregation with a probability of 99% using the Getis-Ord Gi* statistic. The locations and size of the hot spots did not vary in each year. The seven predominant high hot spots for TB were identified in Central and Southeast China, namely, Henan, Hubei,

**Table 3**
Bayesian estimation of sociodemographic and meteorological factors of tuberculosis risk in the elderly in mainland China (excluding Hong Kong, Maco, and Taiwan), 2005-2015.

| Node | Posterior Mean(95%CI) | SD | MC error | Median |
|---|---|---|---|---|
| Intercept | −1.467 (-1.566, 1.393) | 0.053 | 0.006 | −1.464 |
| Time | 0.071 (0.057,0.081) | 0.007 | 0.001 | 0.073 |
| Population density | 0.088 (0.031, 0.129) | 0.022 | 0.003 | 0.090 |
| GDP | −0.046(-0.156, 0.037) | 0.048 | 0.006 | −0.047 |
| Sex ratio(M:F) | 0.162(0.091,0.254) | 0.057 | 0.007 | 0.151 |
| Average humidity | −0.011(-0.043,0.028) | 0.015 | 0.002 | −0.011 |
| Wind speed mean | −0.165(-0.235, 0.108) | 0.033 | 0.004 | −0.167 |
| Average rainfall | 0.095(0.045,0.163) | 0.032 | 0.004 | 0.089 |
| Average Temperature | −0.028(-0.043, 0.018) | 0.021 | 0.003 | −0.041 |

CI = Credible interval.
Mc = Monte Carlo simulation error.
SD = Standard deviation.

Zhejiang, Fujian, and Jiangsu provinces with a 99% probability. The most common cold spots observed in the study period were Heilongjiang and Tibet provinces (Fig. 5). The findings of these hot-spot clusters are similar and support the local spatial autocorrelation (Anselin Moran's I) analysis.

### 3.5. Spatial-temporal regression analysis using the Bayesian CAR model (Ecological study)

A Bayesian model using potential covariates for TB risk in the geriatric population was fitted. The best performing CAR models were selected based on the DIC value. Among the six models that were built, a model with a lower DIC value reflects the best-fit model (Table 2). Accordingly, Model 6, which included a correlated spatial random effect [ui], autoregressive time effect (gi), uncorrelated spatial random effect [vi] and a spatial-temporal interaction random effect [psi], showed a lower DIC value of 1800.

Model **1** (a model with an autoregressive time effect, $\mathbf{g_i}$) and Model **3** (a model including a time trend effect, **time** $_\mathbf{i}$) did not show any significant difference in DIC, which is 36,520. This indicates that adding the time trend effect (**time** $_\mathbf{i}$) had no effect or redundancy on the model.

A model with a low DIC, Model **6**, was initialized and updated including all potential predictor variables into the WinBUGS software (Model S1). The model iteration process clogged at 100,000; this occurred when the kernel density plot showed near normal standard distribution graphs and the autocorrelation plot reached near zero in value. After discarding the first 5000 iterations, each node was set one by one, and the posterior mean was computed. The overall level of the posterior mean of the trend = 0.071 (95% credible interval = 0.057, 0.081). The overall risk effect was significantly different from zero, and it was positive. This indicates that the overall TB risk effect in the elderly would be increasing when all other determinants of TB were constant. Among the covariates considered as TB determinants, the posterior mean for each node with the 95% credible interval is displayed; TB in the elderly was negatively significantly associated with the posterior mean value of -0.028 (95%CI = (-0.043, -0.018), with the average temperature -0.165 (95%CI = (-0.235, -0.108), with the average wind speed -0.046 (95%CI = (-0.156, -0.037), and with the gross domestic product (GDP). These results indicate that the TB risk in the elderly increases with low temperature, gross domestic product and mean wind speed. The average humidity was negatively associated with TB risk in the elderly; however, this result was not significant.

TB was significantly and positively associated with population density at a mean value of 0.088(95%CI = (0.031,0.129), with average rainfall having a mean and 95% credible interval of 0.095(95%CI = (0.045,0.163) and with sex ratio having a mean and 95% credible interval of 0.162(95%CI = (0.091,0.254); these results mean that a one-unit increase in population density would cause an upsurge in the risk of TB in the elderly. Moreover, the TB risk was relatively higher in elderly men (Table 3).

Fig. 6 shows a relative risk choropleth map plot of the TB distribution in the geriatric population in each province. Out of the 31 provinces (excluding Hong Kong, Macao, and Taiwan) in mainland China, 17 provinces exhibited the relative risk of TB to be higher than one. A higher risk of TB was observed in the Central and Southeast provinces of China. The map exceeded the probability (RR > 1) in 17 provinces, namely, Inner-Mongolia, Henan, Hunan, Anhui, Tianjin, Hubei, Liaoning, Fuji, Shandong, Shanxi, Zhejiang, Ningxia, and Jiangsu, etc. (Fig. 6). Provinces with high risk were evident in the same

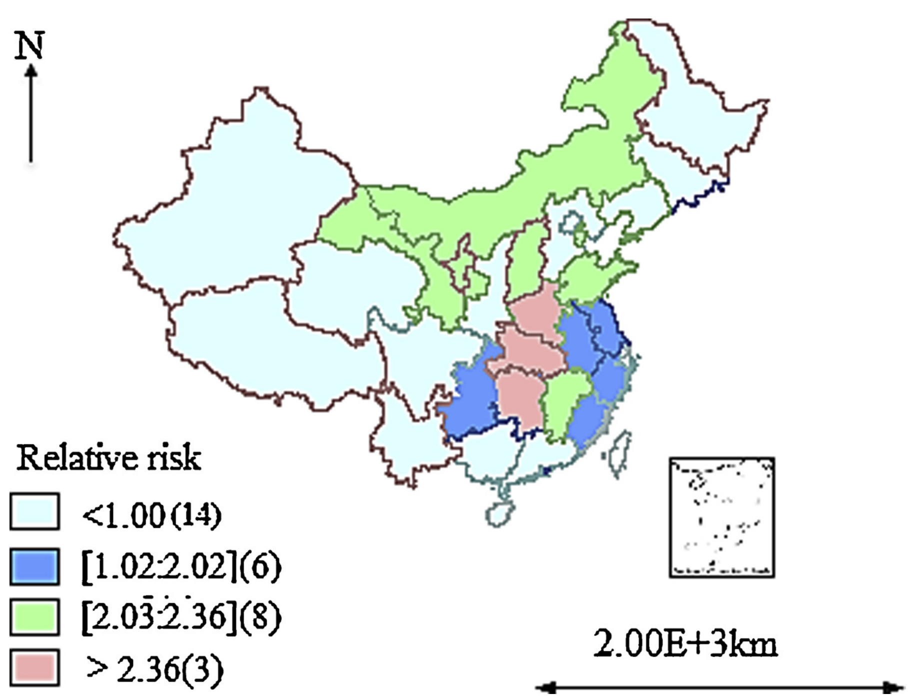


**Fig. 6.** The relative-risk choropleth map plot for tuberculosis in the elderly in China.2005–2015.

**Table 4**
Sensitivity analysis of Bayesian estimation of the sociodemographic and meteorological factors of the tuberculosis risk in the elderly in mainland China (excluding Hong Kong, Maco, and Taiwan), 2005-2015.

| Node | Posterior Mean (95%CI) | SD | MC error | Median |
|---|---|---|---|---|
| Intercept | −1.291 (-1.433, 1.155) | 0.0768 | 0.004303 | −1.288 |
| Time | 0.0117 (-0.01825,0.06489) | 0.02507 | 0.001411 | 0.003421 |
| Population density | 0.0175 (-0.07686,0.1456) | 0.05217 | 0.002909 | 0.016 |
| GDP | −0.2688 (-0.4082, -0.003342) | 0.114 | 0.006402 | −0.3034 |
| Sex ratio(M:F) | 0.0562 (-0.08044, 0.1807) | 0.05931 | 0.003312 | 0.05433 |
| Average humidity | 0.0032 (-0.1224,0.1892) | 0.08679 | 0.00487 | −0.00105 |
| Wind speed mean | −0.0735 (-0.1667,0.1048) | 0.06711 | 0.003758 | −0.08127 |
| Average rainfall | 0.0060 (-0.1076,0.1841) | 0.07318 | 0.004089 | −0.007933 |
| Average temperature | 0.0906 (-0.03576,0.2028) | 0.06306 | 0.003528 | 0.09025 |

CI = Credible interval.
Mc = Monte Carlo simulation error.
SD = Standard deviation.

areas as identified by using LISA analysis in Hunan, Henan and Hubei provinces.

### 3.6. Sensitivity analysis

Sensitivity analysis using the assigned priors for the variance components showed that the Bayesian spatial-temporal analysis for the posterior mean yields almost a robust finding (Table 4).

## 4. Discussion

We explored the space time clusters of TB and the associated factors from 2005 to 2015 at the province level in China using the Bayesian CAR model. Our finding indicates that TB in the geriatric population showed an increasing trend and was geographically aggregated. This trend may be due to the age-related decline in immunity, increasing longevity, poverty, and tobacco smoking in China.

Temporally, the seasonality of TB was observed with peaks in the spring and early summer. This seasonality may be due to the high numbers of TB cases that are infected during the winter and diagnosed in the spring. However, most people want to stay home in the winter, especially when they are sick; however, the photogenic nature of the disease may contribute to diagnosis during the spring. People with low levels of vitamin D are more likely to develop dormant TB and progress to active TB. Older people are prone to developing vitamin D deficiency because of various risk factors, including diminished sunlight exposure and reduced skin thickness (Holick, 1995). Therefore, the TB infection rate is expected to be high in the winter in elderly people, as the cutaneous synthesis of vitamin D is dependent on sunlight. The lack of social support may also contribute to a delay in seeking care after becoming ill, which translates to a delay in diagnosis during the winter (He, 2016). Therefore, this fact may result in an upsurge of diagnosis of TB in the elderly in the spring and continue to the seeking of treatment in summer. Similarly, consistent with earlier studies, seasonal patterns were identified in a study conducted in China (Li et al., 2013), Zhejiang province (Ge et al., 2016), Taiwan (Liao et al., 2012), and India (Thorpe et al., 2004).

Spatially, TB in the geriatric population was geographically aggregated. Identification of 'hot spots' in risk groups (i.e., elderly population) is essential to properly allocate resources and to identify locations for further studies that might inform interventions aimed at reducing the TB burden. The variation in both the incidence and SMR of TB (per 100,000 population) among the provinces was substantial; some provinces reporting a disease incidence several times higher than that of other provinces (up to 12-fold for TB risk). In this study, seven hot-spot areas were identified, namely, Henan, Hubei, Zhejiang, Fujian, Anhui, Hunan, and Jiangsu, which are located in Central and Southeast China. Previously, spatial studies reported similar spatial clustering results in this area (Cao et al., 2016). This clustering may be due to the high population density and high prevalence of drug-resistant TB in these provinces (He et al., 2008). In addition, a study in Zhejiang province revealed that patients with TB had a low level of social support, which may be a significant factor for the burden of TB diseases in the geriatric population in the region (Lin, 2013). Moreover, it is well known that TB 'hot spots' may be common in high burden countries (Ding et al., 2017). China ranks second among 30 high-burden countries in the world (WHO, 2017). In this study, we identified hot-spot areas in the regions with the highest burden in China.

The TB incidence in the geriatric population was not exclusively spatial dependent or time dependent; rather, a spatial-temporal interaction effect was detected. Previous studies presented a spatial-temporal interaction (Pfeiffer et al., 2008; Cao et al., 2016). In this study, a CAR model with a spatial-temporal interaction estimation showed that potential covariates were positively and negatively associated with TB. The temperature and wind could be an influential factor in the risk of TB. The average temperature and wind was negatively associated with TB, which indicated that a one-unit increase in temperature could reduce the risk of TB in the elderly. This result is supported by other research in China (Guo et al., 2017), Nigeria (Omonijo et al., 2011), North India (Narula et al., 2015), Ethiopia (Alene et al., 2017b) and a worldwide study by Yunxia et al. (Liu et al., 2011). In this study, consistent with the findings reported by Cao et al. (2016) and Guo et al. (2017), we found that wind speed was a protective factor for the risk of TB. This may be because cross ventilation is a crucial measure for prevention of pulmonary TB. Therefore, a low speed of wind may contribute to the spread of the bacteria easily floating in the circulating air; thus, poor air circulation prevails and the resistant bacteria can accumulate. Nevertheless, high wind speed could decrease TB by accelerating the air ventilation and reducing people's susceptibility to the bacteria. The average rainfall in this study was significantly associated with TB. Likewise, Guo et al. (2017) and Cao et al. (2016) found that the average rainfall was positively related to TB. The reason might be that high average rainfall leads to increased atmospheric flow, thus helping to spread airborne infections such as TB. Similar to Cao et al. (2016) and Liu et al. (2011), we found a positive relationship of humidity to TB; however, it was not statistically significant.

Health in older age is significantly influenced by economic status and the place of residence. There are large disparities in life expectancy, health status and health service use among older people of low and high socioeconomic status (Liu et al., 2010). In this study, sociodemographic factors, such as population density and sex ratio (M: F), were positively associated with the risk of TB, but GDP was negatively associated with TB in the elderly.

Population density per area (square kilometers) was positively associated with the risk of TB, indicating that a one-unit increase per area (square kilometers) greatly increased the risk of TB. This result is complemented by a study conducted by Alene et al. (Alene et al., 2017a) and Alene et al. (Alene et al., 2017b) in the spatial analysis of tuberculosis in Ethiopia. TB was negatively associated with province-level GDP per capita (10,000 RMB); a one-unit increase in GDP could help to reduce TB. Comparable results were stated in different studies (Guo et al., 2017; Xu et al., 2009). In this study, the risk of TB was higher in elderly males than females. Consistently, the National Tb surveillance in China (Technical Guidance Group of the Fifth National TB Epidemiological Survey and The Office of, Survey FNTE, 2012) in 2010 and other studies by Alene et al. (Alene et al., 2017a), Hsueh et al. (Hsueh et al. (2006)) and Neyrolles et al. (Neyrolles and Quintana-Murci, 2009) all stated higher TB incidences in males. This increased incidence may be due to a higher rate of tobacco use and could be related to the convergence of other risk factors. According to the 2010 Chronic Disease Risk Factor Surveillance Survey (NCCNDC, 2012), the prevalence of smoking in people aged ≥60 years was 22.4%. The prevalence was substantially higher among men (41.5%) than women (4.3%) (National Health and Family Planning Commission of the PRC, 2015).

This study has some limitations. First, while the level of analysis was by province/region, it might be desirable to examine even smaller geographical units, such as districts and cities. However, reliable and comprehensive information at the district/city level is not simply available for both the dependent and independent variables. The other limitation is that our study is based on surveillance data of TB cases, and it may not show the exact ground-level data for the disease. Tuberculosis in the elderly is influenced by a space and time interaction. It shows a clear spatial variation and geographical aggregation. TB in the elderly is a seasonal disease. The geriatric population in areas with high population density, high rainfall, weak wind speed, and low temperature are more likely to develop TB. The GDP is an important factor and is negatively related to TB. TB in the elderly is more pronounced in males than females. This study would provide valuable information for the government to gain a better understanding and identification of the spatial-temporal patterns, relative risk map, regions with a high incidence of risk, and peak seasonal factors to control TB. The commitment of the Chinese government to control and prevent TB should be improved in the screening, early diagnosis, and control of TB in the elderly at the primary care and community health levels.

## Competing interests

The authors declare that they have no competing interests.

## Funding

Our work was supported by the Program of the National Science and Technology Major Project (Serial Number: 2014ZX10004005001).

## Acknowledgments

We acknowledge the Chinese Center for Disease Prevention and Control (CCDC) for the TB data and the China Meteorological Data Sharing Service System for the provision of weather data.

## References

CDC (2016). *CDC | TB | drug-resistant TB.* Cdc.
WHO (2017). *WHO Global tuberculosis report 2017.* World Health Organization Press.
Schaaf, H. S., Collins, A., Bekker, A., & Davies, P. D. O. (2010). Tuberculosis at extremes of age. *Respirology, 15*, 747–763.
Ito, K. (2013). Tuberculosis in the elderly. *The Japanese journal of tuberculosis and chest diseases, 72*(5), 481–490.
Toyota, M., & Sasaki, Y. (2010). [The issue of tuberculosis in the elderly in Japan]. *Kekkaku, 85*(12), 881–894.
Hussein, M. T., Yousef, L. M., & Abusedera, M. A. (2013). Pattern of pulmonary tuberculosis in elderly patients in Sohag Governorate: Hospital based study. *The Egyptian Journal of Chest Diseases and Tuberculosis, 62*(2), 269–274.
World Health Organization (2010). *Global tuberculosis control 2011. Chem Biodivers. 2011.* Geneva: World Health Organization258 WHO/HTM/TB.
Menezes, A. M. B., Hallal, P. C., Perez-Padilla, R., Jardim, J. R. B., Muiño, A., Lopez, M. V., et al. (2007). Tuberculosis and airflow obstruction: Evidence from the PLATINO study in Latin America. *The European Respiratory Journal, 30*(6), 1180–1185.
Pratt, R. H., Winston, C. A., Kammerer, J. S., & Armstrong, L. R. (2011). Tuberculosis in older adults in the United States, 1993-2008. *Journal of the American Geriatrics Society, 59*(5), 851–857.
Rieder, H. L. (1999). (1st Edition). *Epidemiologic basis of tuberculosis controlvol. 73*, Paris Int Union Against Tuberc Lung Dis.17–62.
Davies, P. D. O. (2007). TB in the elderly in industrialised countries. *The International Journal of Tuberculosis and Lung Disease, 11*(11), 1157–1159.
Jovic, D. (2001). The disintegration of Yugoslavia: A critical review of explanatory approaches. *European Journal of Social Theory, 4*, 101–120.
Petersen, P. E. (2003). Tobacco and oral health–the role of the world health organization. *Oral Health & Preventive Dentistry, 1*(4), 309–315.
Ananthakrishnan, R., Kumar, K., Ganesh, M., Kumar, A. M. V., Krishnan, N., Swaminathan, S., et al. (2013). The profile and treatment outcomes of the older (Aged 60 years and above) tuberculosis patients in Tamilnadu, South India. *PLoS One, 8*(7), 6–11.
Velayutham, B. R., Nair, D., Chandrasekaran, V., Raman, B., Sekar, G., Watson, B., et al. (2014). Profile and response to anti-tuberculosis treatment among elderly tuberculosis patients treated under the TB Control programme in South India. *PloS One, 9*(3), e88045.
IHME (Institute for Health Metrics and Evaluation) (2016). *Global burden of disease 2015 data. Global health data exchange.* IHME (Institute for Health Metrics and Evaluation).
Udwadia, Z., & Vendoti, D. (2013). Totally drug-resistant tuberculosis (TDR-TB) in India: Every dark cloud has a silver lining. *Journal of Epidemiology and Community Health, 67*(6), 471–472.
Babu, G. R., & Laxminarayan, R. (2012). The unsurprising story of MDR-TB resistance in India. *Tuberculosis, 92*, 301–306.
Technical Guidance Group of the Fifth National TB Epidemiological Survey, & The Office of, Survey FNTE (2012). The fifth national tuberculosis epidemiological survey in 2010. *Chinese Journal of Antituberculosis,* (34), 485–508.
Abuaku, B., Tan, H., Li, X., Chen, M., & Huang, X. (2010). Treatment default and death among tuberculosis patients in Hunan, China. *Scandinavian Journal of Infectious Diseases, 42*(4), 281–287.
Li, J., Li, T., Du, X., Chung, P.-H., & Zhang, H. (2017). The age-structured incidence and mortality of pulmonary tuberculosis reported in China, in 2005–15: A longitudinal analysis of national surveillance data. *Lancet [Internet],* (Suppl: S12), 390. Available from: https://www.sciencedirect.com/science/article/pii/S0140673617331501.
Zhang, X.-L., Li, S.-G., Li, H.-T., Li, G.-X., Guo, X.-Y., Wang, Y., et al. (2015). Integrating tuberculosis screening into annual health examinations for the rural elderly improves case detection. *The International Journal of Tuberculosis and Lung Disease : the Official Journal of the International Union Against Tuberculosis and Lung Disease, 19*(7), 787–791.
Pfeiffer, D. U., Robinson, T. P., Stevenson, M., Stevens kim, B., Rogers, D. J., & Clements, A. C. (2008). Identifying factors associated with the spatial distrbution of disease. *Spatial Analysis in Epidemiology,* 81–109.
Besag, J., York, J., & Mollie, a. (1991). Bayesian image-restoration, with 2 applications in spatial statistics. *Annals of the Institute of Statistical Mathematics, 43*(1), 1–20.
Clayton, D., & Kaldor, J. (1987). Empirical bayes estimates of age-standardized relative risks for use in disease mapping. *Biometrics, 43*(3), 671.
Knorr-Held, L., & Besag, J. (1998). Modelling risk from a disease in time and space. *Statistics in Medicine, 17*(18), 2045–2060.
Waller, L. A., Carlin, B. P., Xia, H., & Gelfand, A. E. (1997). Hierarchical Spatio-Temporal Mapping of Disease Rates. *Journal of the American Statistical Association, 92*(438), 607–617.
Da, R. D. L., Caccia-Bava, M. D. C. G. G., & Martinez, E. Z. (2012). Spatio-temporal patterns of tuberculosis incidence in Ribeirão Preto, State of São Paulo, southeast Brazil, and their relationship with social vulnerability: A Bayesian analysis. *Revista Da Sociedade Brasileira de Medicina Tropical, 45*(5), 607–615.
Randremanana, R. V., Richard, V., Rakotomanana, F., Sabatier, P., & Bicout, D. J. (2010). Bayesian mapping of pulmonary tuberculosis in Antananarivo, Madagascar. *BMC Infectious Diseases,* 10.
De Queiroz Mello, F. C., Do Valle Bastos, L. G., Machado Soares, S. L., Rezende, V. M. C., Conde, M. B., Chaisson, R. E., et al. (2006). Predicting smear negative pulmonary tuberculosis with classification trees and logistic regression: A cross-sectional study. *BMC Public Health,* 6.
Venkatesan, P. (2008). *Bayesian model*.
Venkatesan, P., Srinivasan, R., & Dharuman, C. (2012). Bayesian conditional auto-regressive model for mapping tuberculosis prevalence in India. *International Journal of Pharmaceutical Sciences and Research, 3*(1), 1–3.
Cao, K., Yang, K., Wang, C., Guo, J., Tao, L., Liu, Q., et al. (2016). Spatial-temporal epidemiology of tuberculosis in mainland China: An analysis based on Bayesian theory. *International Journal of Environmental Research and Public Health, 13*(5).
Alene, K. A., Viney, K., McBryde, E. S., & Clements, A. C. A. (2017a). Spatial patterns of multidrug resistant tuberculosis and relationships to socioeconomic, demographic and household factors in northwest Ethiopia. *PloS One, 12*(2).
Holick, M. F. (1995). Environmental factors that influence the cutaneous production of vitamin D. *The American Journal of Clinical Nutrition, 61*.
He, T. (2016). Social support received by multidrug-resistant tuberculosis patients and related factors : a cross- sectional study in Zhejiang Province, People's Republic of China. *Patient Preference and Adherence,* 1063–1070.
Li, X., Wang, L., Zhang, H., Du, X., Jiang, S., Shen, T., et al. (2013). Seasonal variations in notification of active tuberculosis cases in China, 2005 – 2012. *PloS One, 8*(7), 2005–2012.
Ge, E., Zhang, X., Wang, X., & Wei, X. (2016). Spatial and temporal analysis of tuberculosis in Zhejiang Province, China, 2009-2012. *Infectious Diseases of Poverty, 5*(1),

11. Available from: http://www.idpjournal.com/content/5/1/11.
Liao, C. M., Hsieh, N. H., Huang, T. L., Cheng, Y. H., Lin, Y. J., Chio, C. P., et al. (2012). Assessing trends and predictors of tuberculosis in Taiwan. *BMC Public Health, 12*(1).
Thorpe, L. E., Frieden, T. R., Laserson, K. F., Wells, C., & Khatri, G. R. (2004). Seasonality of tuberculosis in India: Is it real and what does it tell us? *Lancet, 364*(9445), 1613–1614.
He, G. X., Zhao, Y. L., Jiang, G. L., Liu, Y. H., Xia, H., Wang, S. F., et al. (2008). Prevalence of tuberculosis drug resistance in 10 provinces of China. *BMC Infectious Diseases,* 8.
Lin, Y. (2013). *Seasonal dynamics of tuberculosis epidemics and implications for multidrug-resistant infection risk assessment.* 1–13.
Ding, P., Li, X., Jia, Z., & Lu, Z. (2017). Multidrug-resistant tuberculosis (MDR-TB) disease burden in China: A systematic review and spatio-temporal analysis. *BMC Infectious Diseases, 17*(1).
Guo, C., Du, Y., Shen, S. Q., Lao, X. Q., & Qian, J. (2017). *Spatiotemporal analysis of tuberculosis incidence and its associated factors in mainland China*.
Omonijo, A. G., Oguntoke, O., Matzarakis, A., & Adeofun, C. O. (2011). A study of weather related respiratory diseases in eco-climatic zones. *African Review of Physics, 5*, 41–56.
Narula, P., Sihota, P., Azad, S., & Lio, P. (2015). Analyzing seasonality of tuberculosis across Indian states and union territories. *Journal of Epidemiology and Global Health, 5*(4), 337–346.
Alene, K. A., Viney, K., Mcbryde, E. S., & Clements, A. C. A. (2017b). *Spatiotemporal transmission and socio-climatic factors related to paediatric tuberculosis in north-western Ethiopia co m m er c ia l u se on on c l u.* 12.
Liu, Y., Jiang, S., Liu, Y., Wang, R., Li, X., Yuan, Z., et al. (2011). Spatial epidemiology and spatial ecology study of worldwide drug-resistant tuberculosis. *International Journal of Health Geographics, 10*(1), 50. Available from: http://ij-healthgeographics.biomedcentral.com/articles/10.1186/1476-072X-10-50.
Liu, J., Chen, G., Chi, I., Wu, J., Pei, L., Song, X., et al. (2010). Regional variations in and correlates of disability-free life expectancy among older adults in China. *BMC Public Health,* 10.
Xu, W., Lu, W., Zhou, Y., Zhu, L., Shen, H., & Wang, J. (2009). Adherence to anti-tuberculosis treatment among pulmonary tuberculosis patients: A qualitative and quantitative study. *BMC Health Services Research, 9*(1), 169. Dec18 [cited 2018 Apr 13], Available from: http://www.ncbi.nlm.nih.gov/pubmed/19765290.
Hsueh, P. R., Liu, Y. C., So, J., Liu, C. Y., Yang, P. C., & Luh, K. T. (2006). Mycobacterium tuberculosis in Taiwan. *The Journal of Infection, 52*, 77–85.
Neyrolles, O., & Quintana-Murci, L. (2009). Sexual inequality in tuberculosis. *PLoS Medicine, 6*.
National Health and Family Planning Commission of the PRC (2015). *World health Organization1. Ageing. 2. Delivery of health care. 3. Aged. 4. National health programs. 5. Health services for the aged. 6. China. I*World Health Organization I 978 92 4 150931 2 (NLM classification: W 104) © WHO. China country assessment report on ageing and health [Internet]. Available from: www.who.int) or.